International Journal of Food Microbiology 385 (2023) 110011

Contents lists available at ScienceDirect

International Journal of Food Microbiology

journal homepage: www.elsevier.com/locate/ijfoodmicro

# Biofilm formation, sodium hypochlorite susceptibility and genetic diversity of *Vibrio parahaemolyticus*

Dan Wang [a], Graham C. Fletcher [b], Stephen L.W. On [c], Jon S. Palmer [a], Dragana Gagic [d], Steve H. Flint [a,*]

[a] School of Food and Advanced Technology, Massey University, Private Bag 11222, Palmerston North, New Zealand
[b] The New Zealand Institute for Plant & Food Research Limited, Private Bag 92169, Auckland 1142, New Zealand
[c] Faculty of Agriculture and Life Sciences, Lincoln University, Private Bag 85084, Canterbury, New Zealand
[d] School of Fundamental Sciences, Massey University, Private Bag 11222, Palmerston North, New Zealand

ARTICLE INFO

*Keywords:*
Biofilm
Sodium hypochlorite
Whole genome sequencing (WGS)
Genomic feature
Multilocus sequence typing (MLST)

ABSTRACT

*Vibrio parahaemolyticus* is a marine oriented pathogen; and biofilm formation enables its survival and persistence on seafood processing plant, complicating the hygienic practice. The objectives of this study are to assess the ability of *V. parahaemolyticus* isolated from seafood related environments to form biofilms, to determine the effective sodium hypochlorite concentrations required to inactivate planktonic and biofilm cells, and to evaluate the genetic diversity required for strong biofilm formation. Among nine isolates, PFR30J09 and PFR34B02 isolates were identified as strong biofilm forming strains, with biofilm cell counts of 7.20, 7.08 $\log_{10}$ CFU/cm$^2$, respectively, on stainless steel coupons after incubation at 25 °C. Free available chlorine of 1176 mg/L and 4704 mg/L was required to eliminate biofilm cells of 1.74–2.28 $\log_{10}$ CFU/cm$^2$ and > 7 $\log_{10}$ CFU/cm$^2$, respectively, whereas 63 mg/L for planktonic cells, indicating the ineffectiveness of sodium hypochlorite in eliminating *V. parahaemolyticus* biofilm cells at recommended concentration in the food industry. These strong biofilm-forming isolates produced more polysaccharides and were less susceptible to sodium hypochlorite, implying a possible correlation between polysaccharide production and sodium hypochlorite susceptibility. Genetic diversity in *mshA, mshC* and *mshD* contributed to the observed variation in biofilm formation between isolates. This study identified strong biofilm-forming *V. parahaemolyticus* strains of new multilocus sequence typing (MLST) types, showed a relationship between polysaccharide production and sodium hypochlorite resistance.

## 1. Introduction

*V. parahaemolyticus* is a Gram-negative bacterium that naturally exists in aquatic environments and seafood, such as oyster, clam, mussel, octopus, shrimp, crab and fish. The infections are associated with consumption of raw or undercooked seafood. It grows substantially when temperatures exceed 14–19 °C and is prevalent during the summer and autumn seasons (Baker-Austin et al., 2010; Cruz et al., 2015). In the United States, the average annual number of *Vibrio* infections increased by 54 % between 2006 and 2017, and by 79 % in 2019 (Abanto et al., 2020). The Cholera and Other *Vibrio* Illness Surveillance System in the United States received 4116 reports of *V. parahaemolyticus* infections between 2010 and 2018 (CDC, 2021). In China, they experience an average of 523.5 cases each year during 2010 and 2020 (FAO, 2021). Climate change has been proposed as an explanation for the global spread of *V. parahaemolyticus* infections. Outbreaks have been regularly reported in countries with no or sporadic incidence in Canada, the United Kingdom, France, North Europe, New Zealand and Australia (Baker-Austin et al., 2020; Baker-Austin et al., 2018), raising concerns in the food industry.

There have been 5149 *V. parahaemolyticus* isolates submitted to the Molecular Typing and Microbial Genome Diversity (PubMLST) Database by February 2022 (Jolley et al., 2018). Some pandemic clones are more virulent than others and have been implicated in several previous outbreaks. Sequencing type 3 (ST3) emerged in Asia in the mid-1990s and spread throughout the world, becoming the most common pandemic clone by 2012 (Nair et al., 2007). Sequencing type 36 (ST 36) strains were restricted to the Pacific Northwest and Canada (Daniels et al., 2000), but have spread further into Europe, involving the largest known food-borne *Vibrio* outbreak reported in Spain in 2012 (Martinez-Urtaza

* Corresponding author.
*E-mail address:* s.h.flint@massey.ac.nz (S.H. Flint).

https://doi.org/10.1016/j.ijfoodmicro.2022.110011
Received 28 August 2022; Received in revised form 19 October 2022; Accepted 3 November 2022
Available online 8 November 2022

et al., 2018). ST 36, according to Abanto et al. (2020), can disperse intercontinentally due to its highly pathogenic and persistent nature, posing a threat to the safety of seafood products and human health. The epidemiology of *V. parahaemolyticus* infections has shifted from the dominance of domestically redistricted strains to the transcontinental spread of new clones. However, the relationship between ST and biofilm-forming ability of *V. parahaemolyticus* is unknown.

Biofilm formation is a dynamic life cycle involving motility, attachment, biofilm production and dispersal; once biofilm develops, the endurance and environmental adaptability enable cells to survive environmental stress. *V. parahaemolyticus* as a biofilm have advantages in seafood environments. *V. parahaemolyticus* biofilm is assisted by a dual flagellar system - polar and lateral flagella (Kim and McCarter, 2000), which is not the case with *Escherichia coli*, *Salmonella* spp. and *Listeria monocytogenes* pathogens. *V. parahaemolyticus* can produce an active chitinase, enabling it to adsorb onto chitin- and copepod- surfaces (e.g. oysters, clams, fish, shrimp, and mussels, etc.) (Kaneko and Colwell, 1975). This helps *V. parahaemolyticus* initiate colonization of seafood due to the capability to degrade and utilize chitinous materials of seafood surfaces. *V. parahaemolyticus* biofilms form on stainless steel, polystyrene, glass, and other abiotic surfaces in food processing equipment and packaging materials, showing a higher resistance than their planktonic counterparts, to cleaning and sanitation that may lead to recurring contamination.

Chlorine-based disinfectants, such as sodium hypochlorite, are oxidizing agents widely used for cleaning and disinfection in the food industry due to low cost, easy-use and broad-spectrum bactericidal activities. Although the concentrations of disinfectants required to eliminate biofilm cells have been determined in many species such as L. *monocytogenes* (Cruz and Fletcher, 2012) and *Pseudomonas fluorescens* (Cai et al., 2019), information gaps remain in the response of *V. parahaemolyticus* biofilm cells to sodium hypochlorite that may be used in the seafood processing environment (Wang et al., 2022). Sodium hypochlorite at recommended concentrations is inadequate to inactivate *V. parahaemolyticus* so optimisation of treatment with sodium hypochlorite is required. Shikongo-Nambabi et al. (2010) found that when exposing mature *V. parahaemolyticus* biofilms for 1 h with sodium hypochlorite (4 mg/L free available chlorine pH not specified), the bacterial density decreased from 7.90 to 3.97 $\log_{10}$ CFU/cm$^2$. Another study examined the efficacy of sodium hypochlorite in reducing the bacterial population of *V. parahaemolyticus* in mature biofilms formed on stainless steel, glass, and polystyrene, and discovered that a 10-min treatment with sodium hypochlorite (20 mg/L available chlorine, pH not specified) could reduce cell populations by as much as 3.0 $\log_{10}$ CFU/cm$^2$ from 5.5 $\log_{10}$ CFU/cm$^2$ (Rosa et al., 2018). However, information gaps remain in these studies, in particular with reference to the pH and temperatures used. Firstly, sodium hypochlorite dissolved in water will raise the pH and reduce antimicrobial efficacy. In the food industry, it has been recommended to adjust pH of sodium hypochlorite solution to 6.5–7.0 before the use on food contact surfaces. However, pH of sodium hypochlorite solution was overlooked when killing biofilm cells in the above studies. Additionally, sodium hypochlorite efficacy for removing biofilm cells will depend on amount and nature of biofilm formation of *V. parahaemolyticus*.

Despite widespread awareness of *V. parahaemolyticus* control in seafood, there is a lack of understanding around *V. parahaemolyticus* biofilm development and its resistance to sodium hypochlorite, particularly regarding the relationship between the phenotype and genotype. Thus, the objectives of this study are to: (1) assess the ability of *V. parahaemolyticus* isolates from different clones to form biofilms; (2) determine the susceptibility of *V. parahaemolyticus* biofilm cells to sodium hypochlorite; and (3) decipher the genotype profiles of strong biofilm formers using whole genome sequencing (WGS).

## 2. Material and methods

### 2.1. Bacterial isolates and culture conditions

Nine *V. parahaemolyticus* strains were used in this study, seven of them were isolated from New Zealand shellfish (isolation using alkaline peptone water of pH 8.6–9.0) and were kindly provided by The New Zealand Institute for Plant and Food Research Ltd. Another two strains are clinical isolates, PFR37D08 (National Health Index (NHI) No. 75/0294) and PFR37E03 (NHI No. CHE2822), provided by the Institute of Environmental Science and Research (ESR), New Zealand.

Strains were stored at −80 °C using the low temperature bead storage system (Protect; Thermo Fisher Scientific, USA). To recover, a bead was picked using a needle aseptically, transformed into tryptic soy broth (TSB) broth with 3 % NaCl and incubated at 37 °C with shaking at 120 rpm till cells enter stationary-phase (5–8 h). Cultures were centrifuged (10,000 rpm, 5 min) and washed for three times using sterile PBS buffer, the harvested cells were ready for use.

### 2.2. Motility assay

Swimming and swarming motility of *V. parahaemolyticus* were measured as described previously by Sybiya Vasantha Packiavathy et al. (2012) with minor modifications. Briefly, swimming motility was characterized on agar plates containing 0.3 % agar, 1 % tryptone and 1 % NaCl; and swarming motility was on agar plates containing 0.5 % agar, 0.8 % tryptone, 1 % NaCl and 0.5 % glucose. Cell suspension (5 μL) of *V. parahaemolyticus* ($OD_{595} = 0.4 \pm 0.05$) was stabbed into the centre of media plates, and the motility was evaluated by determining the migration of *V. parahaemolyticus* from the centre to the periphery of the plate after incubation at 37 °C for 18 h.

### 2.3. Crystal violet assay

A cell suspension was diluted to obtain an $OD_{595}$ (Absorbance measurements at 595 nm) of 0.15 ± 0.05 using a microplate reader (Varioskan Lux 3020–1333, Thermo Fisher, USA), and each 200 μL of cell culture was added into the well of a 96-well flat-bottom microtiter plate. The plate was incubated at 37 °C for 72 h, then the $OD_{595}$ was examined. The plate was inverted to remove the cultures, and each well was washed three times using 230 μL of distilled water, followed by 230 μL of ethanol to fix the cells for 10 min. The ethanol was removed, and the plate was allowed to dry. Then, each well was stained with 230 μL of 2 % crystal violet (CV) for 10 min, washed three times using distilled water, followed by 210 μL of 33 % acetic acid added into each well to dissolve the CV stain. The absorbance of resulting solution in each well was measured at 570 nm, and the biofilm forming index (BFI) of each strain was evaluated using the following equation:

$$BFI = \frac{(OD_{570} - OD_{570con})}{(OD_{595} - OD_{595con})}$$

$OD_{570}$ and $OD_{595}$ represent the absorbance value of sample wells at 570 nm and 595 nm, respectively. $OD_{570con}$ and $OD_{595con}$ represent the absorbance value of wells with only TSB with 3 % NaCl as a blank. The degree of biofilm formation was classified according to Naves et al. (2008): strong (BFI ≥ 1.10), moderate (1.09 ≥ BFI ≥ 0.70), weak (0.69 ≥ BFI ≥ 0.35) and none (BFI < 0.35).

### 2.4. Biofilm development on stainless steel surface and cells enumeration

Prepared cell culture (1 mL, ~ 4 $\log_{10}$ CFU/mL) was pipetted into each well of 48-well flat-bottom polystyrene plates, along with one precleaned and sanitised stainless-steel coupon (304 stainless steel, 1 × 1 cm). The number of culturable cells in the biofilm matrix was determined using a bead vortex mixing method reported previously with minor modifications (Hayrapetyan et al., 2015). In short, each coupon

was rinsed three times using sterile distilled water to remove the planktonic cells and transferred into a 25 mL glass bottle filled with 10 mL of 0.1 % peptone buffered water and 5 g of glass beads (5–8 mm), followed by 1 min vortex mixing to disrupt the biofilm matrix from the stainless steel surface and obtain individual cells. 10-fold serial dilutions of biofilm cell solution were prepared and colony forming unit (CFU) enumeration was examined on 3 % NaCl tryptic soy agar (TSA) plates.

### 2.5. Susceptibility to sodium hypochlorite

Sodium hypochlorite solution was prepared aseptically and used within 20 min. In brief, commercial concentrated sodium hypochlorite (XY-12, ECOLAB, New Zealand) containing around 140 g/L available chlorine (147 g/L sodium hypochlorite) was diluted in distilled water and the pH was adjusted to a range of 6.7 to 6.9 using 1 M HCl. The amount of free chlorine in the sodium hypochlorite solution was determined using titration (Zheng and Brook, 2021).

To determine the sodium hypochlorite susceptibility of planktonic *V. parahaemolyticus* cells, each well of 96-well polystyrene plates were loaded with 180 μL cell suspension (~ 8 $\log_{10}$ CFU/mL) and 20 μL sodium hypochlorite solution. The reaction was neutralised with 50 μL of 1 % sodium thiosulfate after 5 min cells exposure to sodium hypochlorite. Each set of experiments included a positive control (180 μL of inoculum and 20 μL distilled water) as well as a negative control (180 μL of saline and 20 μL of sodium hypochlorite). 10-fold serial dilutions of cells were prepared and colony forming unit (CFU) enumeration was examined on 3 % NaCl TSA plates. To determine the sodium hypochlorite susceptibility of *V. parahaemolyticus* biofilm cells, coupons containing pre-formed biofilm were placed into 48-well flat-bottom polystyrene plates. 1 mL of sodium hypochlorite solution was pipetted into each well, containing a coupon for 5 min, and then the coupon was transferred to another well containing 1 % sodium thiosulfate to neutralise the sodium hypochlorite. Cells on stainless steel coupons were detached and counted as described earlier.

### 2.6. Fluorescence microscopy

To visualise the biofilm, coupons with cultured biofilms were rinsed with sterile distilled water three times and allowed to half dry on a glass microscope slide. To stain, 1 drop of calcofluor white stain was placed on each coupon and left for 1 min before washing with sterile distilled water and allowing to partially dry. The stained samples were examined using an epifluorescent microscope (BX53; Olympus Corp., Japan) equipped with a DAPI filter (excitation at 340–360 nm, emission at 410 nm), the images were captured by the cellSense Dimension programme.

### 2.7. Detection of biofilm forming related genes

The Centre for Environment, Fisheries, and Aquaculture Science (CEFAS) did the DNA extraction, library construction and whole genome sequencing of *V. parahaemolyticus* using MiSeq with a coverage of 40-120× (Baker-Austin et al., 2020). Clean reads were used for de novo assembly and annotation via the Bactopia pipeline using Velvet and SPADES as the assembler (Petit and Read, 2020). The quality of assembled contigs was assessed using QUAST and CheckM (Gurevich et al., 2013; Parks et al., 2015). Genes related with colonization, toxin production, EPS biosynthesis and Type II secretion system were selected to detect the genetic diversity in *V. parahaemolyticus* (Table 2). The amino acid sequences of *V. parahaemolyticus* RIMD 2210633 were retrieved from the National Centre for Biotechnology Information (NCBI) Database and selected as the reference genome, followed by copying into a local database for BLASTP searching via diamond (Buchfink et al., 2021). Each sequenced *V. parahaemolyticus* genome was searched to identify the presence of genes (with >70 % identity and > 70 % sequence coverage) (Fang et al., 2022). The draft genomes were submitted to GenBank under the BioProject PRJNA808748 https://dataview.ncbi.nlm.nih.gov/object/PRJNA808748?reviewer=26p271csjvbj6lm07mvgldooc.

### 2.8. Statistical analysis

All experiments were performed with two or three biological replicates and three technical replicates. One-way variance analysis (ANOVA) was generated to evaluate the significant differences among experimental results with a $p$ value below 0.05 considered as statistically significant.

## 3. Results

### 3.1. Ability of V. parahaemolyticus to swim and swarm

The diameter of the migration on the agar plate reflected the ability of *V. parahaemolyticus* to swim and swarm (Table 3). Each of the nine strains demonstrated swimming ability, with the top three measuring 71.00 ± 15.56 mm (strain PFR30G02), 69.33 ± 17.48 mm (strain PFR21C03) and 58.58 ± 30.50 mm (strain PFR30J09). With a diameter of 10.33 ± 0.76 mm, strain PFR34B02 exhibited the least capacity to swim. In the swarming motility assay, strain PFR29A04 had the lowest value of 22.83 ± 5.97 mm and strain PFR30J09 had the highest value of 60.33 ± 8.25 mm.

### 3.2. Ability of V. parahaemolyticus to form biofilm

The CV assay and the BFI value revealed that PFR30J09 and PFR34B02 formed the best biofilms, with BFI values of 1.214 and 1.060, respectively (Fig. 1). Biofilm formation varies and a comparison between the good and poor biofilm formers may reveal the important factors in biofilm formation. For other strains, the crystal violet staining and BFI values were high in PFR29A04 and PFR37D08, and low for PFR21C03, PFR24B07 and PFR37C06. Significant differences ($p < 0.05$) were observed between means of the good and poor biofilm isolates.

Biofilm formation by *V. parahaemolyticus* on stainless steel coupons is shown in Fig. 2. The detectable populations of *V. parahaemolyticus* in the biofilm matrix increased from ~4 $\log_{10}$ CFU/cm$^2$ to ~7 $\log_{10}$ CFU/cm$^2$ at 25 °C within 24 h. Strains PFR30J09 and PFR34B02 formed the best biofilms based on cell numbers with most reaching a maximum of 7.08–7.20 $\log_{10}$ CFU/cm$^2$. The PFR30J09 population increased from 3.83 $\log_{10}$ CFU/cm$^2$ at the first hour to 7.20 $\log_{10}$ CFU/cm$^2$ by the 6th hour. The cell numbers of PFR34B02 increased from 3.46 $\log_{10}$ CFU/cm$^2$ at the first hour to 7.08 $\log_{10}$ CFU/cm$^2$ 6th hour. For PFR37D08 and PFR37E03, an apparent delay in the onset of biofilm formation was detected (growth curve peaked at 11th hour), indicating a long lag phase in biofilm growth. PFR37D08, PFR37E03 and PFR21C03 produced the lowest number of biofilm cells.

The polysaccharide content and the biofilm matrix were visualized using epifluorescence microscopy following calcofluor white staining. *V. parahaemolyticus* on stainless-steel coupons was stained after 6 h incubation at 25 °C. The most biomass was produced by PFR30J09 and PFR34B02 with dense and strong blue fluorescence (Fig. 3). Other strains had a flat and loose sessile cell distribution with fewer cell clusters. The microscopic result was consistent with other biofilm assays.

### 3.3. Susceptibility of planktonic and biofilm cultures to sodium hypochlorite

Planktonic cells were reduced by approximately 0.9 $\log_{10}$ CFU/mL with 16 mg/L chlorine and they were reduced by 1.49–2.79 $\log_{10}$ CFU/mL with 35 mg/L chlorine (Fig. 4). There was variation in the chlorine sensitivity of different strains with 35 mg/L chlorine, with PFR30J09 and PFR37E03 producing low reductions of 1.76 and 1.49 $\log_{10}$ CFU/mL, respectively, whereas PFR21C03, PFR37C06, and PFR37D08

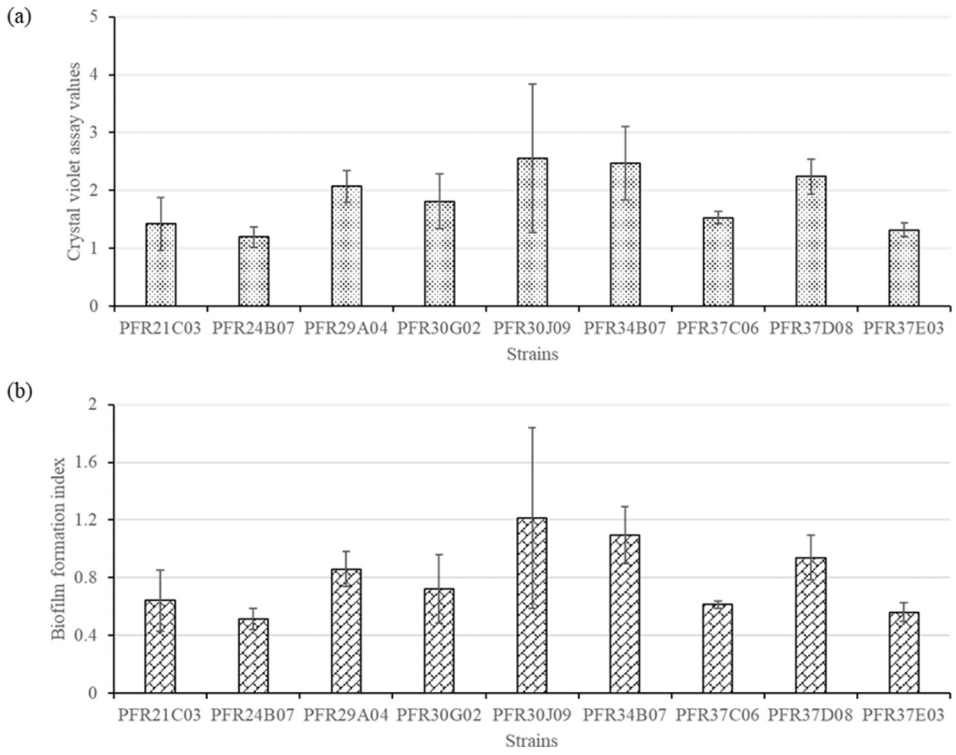


**Fig. 1.** Biofilm forming ability of *V. parahaemolyticus* strains. (a) presented the crystal violet values within 9 *V. parahaemolyticus* isolates. (b) shows their biofilm formation index (BFI) results (Mean ± SD).

reduced by 2.33, 1.81, and 2.24 $\log_{10}$ CFU/mL, respectively. Following exposure to 63 mg/L chlorine, all *V. parahaemolyticus* planktonic cells decreased to undetectable levels on agar plates, a reduction of >7 $\log_{10}$ CFU/mL.

Biofilms of *V. parahaemolyticus* required a chlorine concentration roughly 75 times greater than that needed for planktonic cells, to decrease the culturable cells to undetectable levels using the CFU counting method (Fig. 5). A concentration of 1176 mg/L chlorine was required to lower the *V. parahaemolyticus* culturable cell populations on stainless steel coupons by 1.74–2.28 $\log_{10}$ CFU/cm$^2$. The smallest declines were observed in the PFR30J09 and PFR34B02 biofilms, with cell populations decreasing by 1.78 and 1.91 $\log_{10}$ CFU/cm$^2$, respectively. When biofilms were treated with 4704 mg/L chlorine, the cell population of all strains except PFR30J09 and PFR34B02 was reduced to undetectable levels.

### 3.4. Analysis of genetic diversity

The clinical isolates PFR37D08 and PFR37E03 had the *tdh* gene that encodes thermostable direct hemolysin (TDH) toxins whereas other stains did not, while all nine isolates had the *tlh* gene encoding thermolabile hemolysin (TLH). Genes common among the isolates were those responsible for CPS polysaccharide biosynthesis, *syp*-like polysaccharide biosynthesis, chitin-regulated pili assembly, Type II secretion system and colonization factor GbpA There were differences among sequenced genomes located in genes of *mshA*, *mshC* and *mshD* that contribute to attachment and biofilm formation in *V. parahaemolyticus* (Fig. 6). Strain PFR21C03, PFR30G02, PFR37D08 and PFR37E03 lacked these three genes, among which, PFR21C03 and PFR37E03 were identified as weak biofilm forming strains. The strong biofilm-forming strain PFR30J09 and an intermediate one PFR37C06 possessed all these three genes, meanwhile, intermediate biofilm-forming strain PFR24B07 and strong biofilm former PFR34B02 had *mshC* and *mshD*. Strain PFR29A03 had the sole gene of *mshA*.

Combining information from Table 1, PFR37D08 of ST36 was identified as a weak biofilm former though it is the most prevalent environmental pathogen. Strain PFR30J09 and PFR37C06 shared the same nearest ST type of 2650, however, PFR30J09 was identified as the strong biofilm former whereas PFR37C06 was not. Strain PFR34B02 of potential ST 2648 was another strong biofilm forming strain.

## 4. Discussion

The persistence of the *V. parahaemolyticus* biofilm in seafood processing plants may result in pathogen recurrence and complicate hygienic treatment. In the present study, *V. parahaemolyticus* biofilms required 75 times higher disinfectant concentrations than planktonic cells, which raises concerns about developing and optimising biofilm control strategies. This study advances our understanding of the phenotypic and genetic interactions underlying *V. parahaemolyticus* biofilm development, meanwhile demonstrated promising ways to inhibit attachment of *V. parahaemolyticus* to surfaces via interfering with the Mannose-sensitive hemagglutinin (MSHA) type IV pilus. This study also identified two strains of novel MLST ST types that showed strong biofilm on stainless steel, but whether they will remain strong on other surfaces requires further investigation.

*V. parahaemolyticus* possesses dual flagella, polar flagella for swimming and lateral flagella for swarming. The extent to which bacteria swim and swarm contributes to the initial attachment and development of biofilm structures (Wadhwa and Berg, 2022). However, in our study, no strong links between swimming, swarming motility, and ability to form biofilms were seen in our study ($r = 0.063$ and 0.016, respectively; Table 3), implying swimming and swarming contribute to but did not play essential roles in biofilm formation. Other motility modes, other than swimming and swarming, for instance, twitching and gliding motility may be present in *V. parahaemolyticus* but were not examined in our study. This result is consistent with prior findings demonstrating that motility is not strongly associated with the ability to produce biofilms. Mizan et al. (2016) reported a weak negative correlation (−0.124) between swarming motility and biofilm formation in *V. parahaemolyticus*

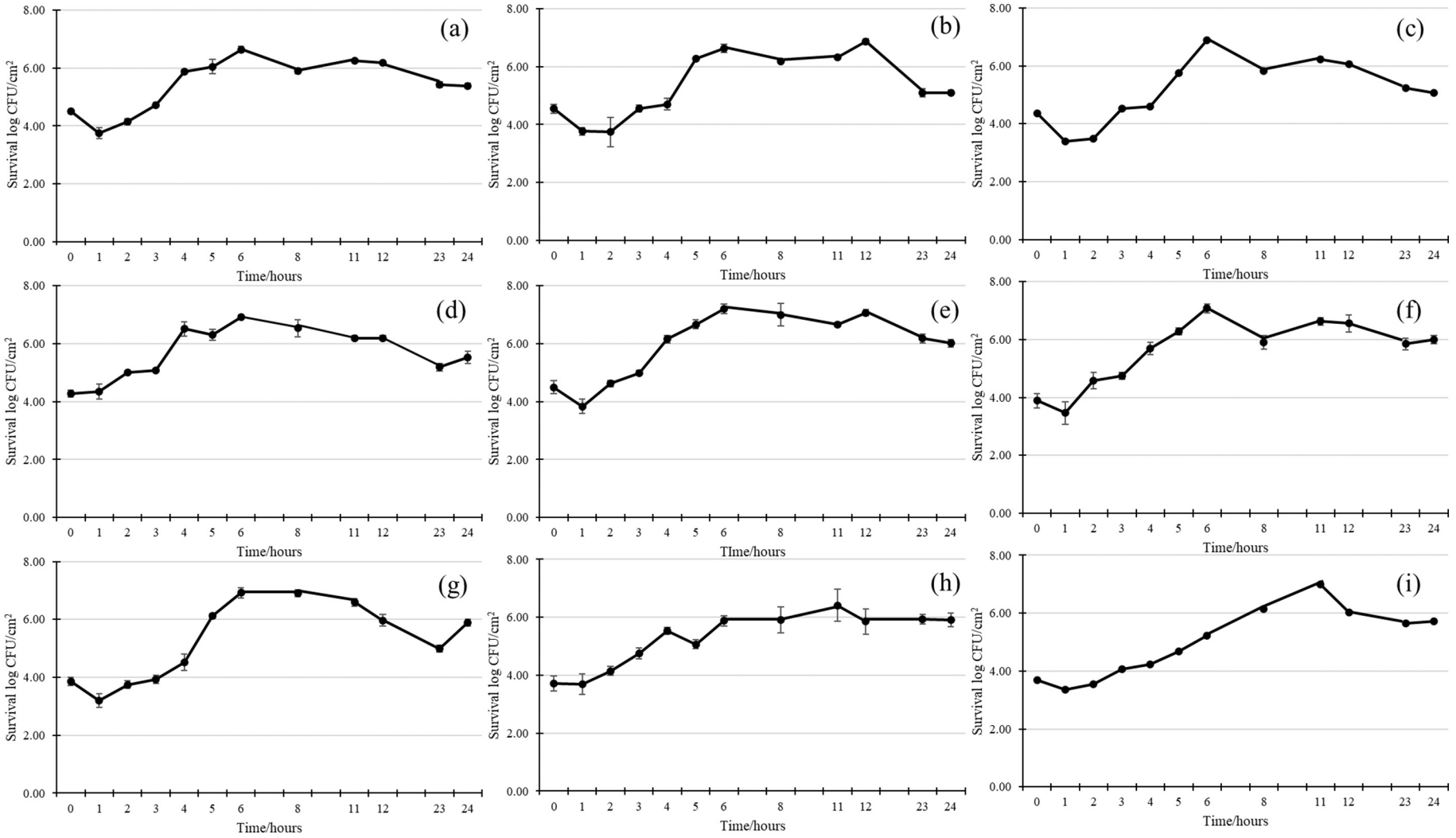


**Fig. 2.** *Vibrio parahaemolyticus* growth on stainless steel coupons within 24 h at 25 °C (Mean +/− SD). The indications for strains are as follows: (a) PFR21C03, (b) PFR24B07, (c) PFR29A04, (d) PFR30G02, (e) PFR30J09, (f) PFR34B02, (g) PFR37C06, (h) PFR37D08 and (i) PFR37E03.

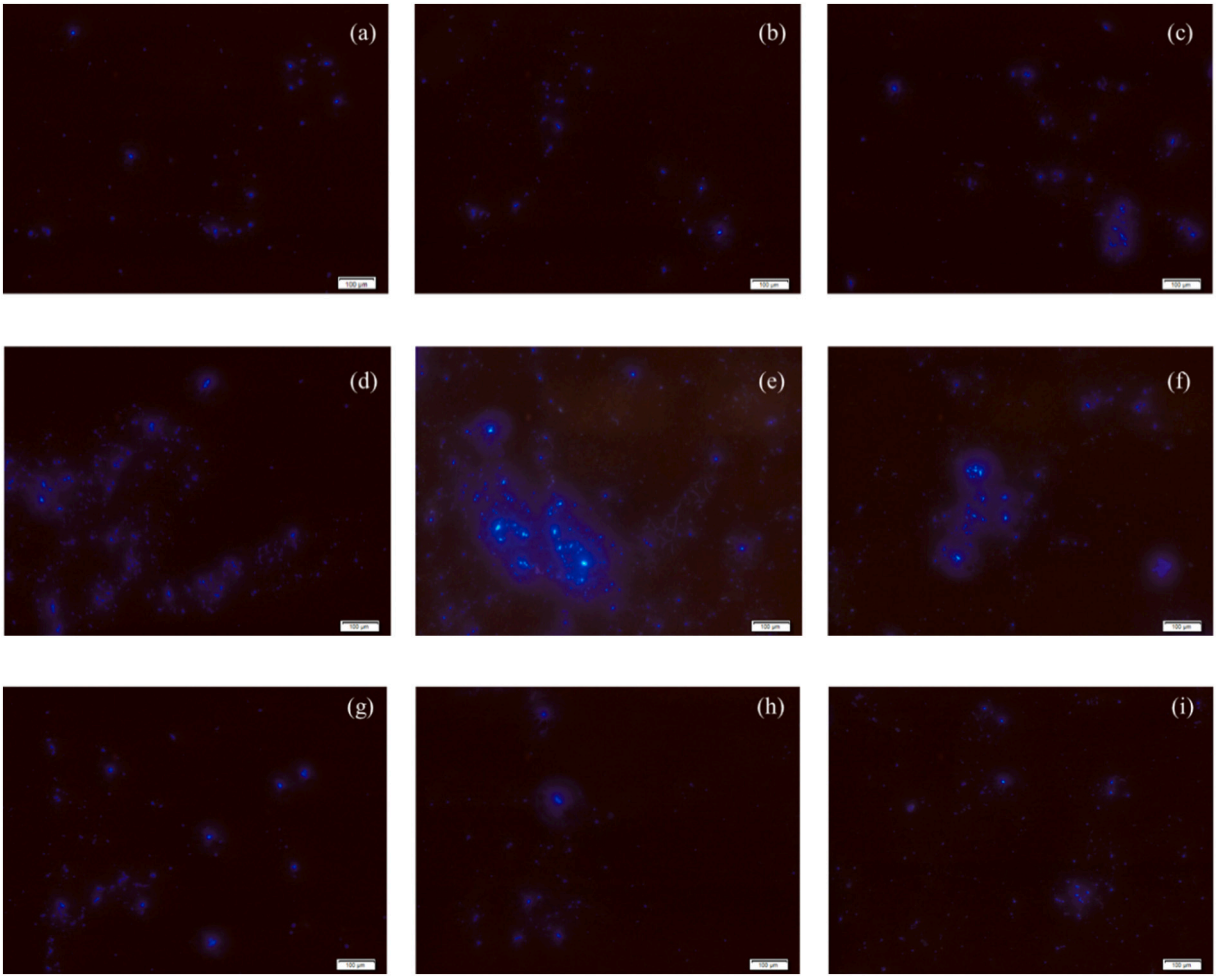


**Fig. 3.** Epifluorescence microscope screen of sessile *V. parahaemolyticus* (6-hour old, 25 °C) on stainless steel. Blue fluorescence was emitted from calcofluor white stain when binding with polysaccharides in biofilms. The indications for strains are as follows: (a) PFR21C03, (b) PFR24B07, (c) PFR29A04, (d) PFR30G02, (e) PFR30J09, (f) PFR34B02, (g) PFR37C06, (h) PFR37D08 and (i) PFR37E03.

isolates, as well as a moderate positive association between swimming motility and biofilm formation. No correlation was concluded between motility and biofilm production in L. *monocytogenes* as reported by Di Bonaventura et al. (2008), regardless of multiple temperatures tested. Sheikh et al. (2001) suggested that the absence of motility in *Escherichia coli* did not impair the ability to produce biofilms.

The BFI is normally determined to demonstrate biofilm-forming ability using the microtiter plate assay (Lucero-Mejia et al., 2020). In this study, BFI results suggested that PFR30J09 and PFR34B02 produce strong biofilm, whereas PFR21C03, PFR37C06 and PFR37E03 produce weak biofilm. PFR37D08 produced weak cell growth on stainless steel but showed a relatively high crystal violet value on polystyrene. This may be a result of the surface used with polystyrene favouring PFR37D08 rather than stainless steel. As the crystal violet stain will stain dead and live cells the standard test on polystyrene may simply reflect the difference between live sells (on stainless steel) compared with dead and live cells (on polystyrene) (Chiba et al., 1998). Ideally a crystal violet test should also be done on the stainless steel surfaces to determine if the observation is due to the nature of the substrate or the difference in test methods.

Stainless steel is one of the most frequently used surfaces in the food industry. In this study, CFU enumeration was used to detect viable and countable *V. parahaemolyticus* cells living in biofilms on stainless steel coupons. PFR30J09 and PFR34B02 formed the most biofilms. The population in PFR30J09 biofilm rose from 3.83 to 7.20 $\log_{10}$ CFU/$cm^2$ and the population of PFR34B02 increased from 3.46 to 7.08 $\log_{10}$ CFU/$cm^2$ within 6 h. The weak biofilm formers, such as PFR37D08, had growth curves with a delay in the rise of cell counts. Calcofluor white stain can bind to β-linked polysaccharides and emit blue fluorescence. Epifluorescence microscopy provided a direct, visual approach to define microbial biofilm forming ability. PFR30J09 and PFR34B02 were confirmed as strong biofilm forming strains under epifluorescence microscopy, with dense cell clusters and a structured matrix, whereas others showed flat and loose cell clusters. Using multiple assays for biofilm formation, the results were consistent for PFR30J09 and PFR34B02 therefore these were chosen as the strong biofilm formers for this study, PFR21C03 and PFR37D08 were selected as the weak biofilm strains for this study.

Studies on the inactivation of *V. parahaemolyticus* are limited. In this study, the effective chlorine concentration required to kill biofilm of *V. parahaemolyticus* was approximately 75-fold higher than that required to kill planktonic counterparts. In one published study, *V. parahaemolyticus* planktonic culture was reduced by 2.2 $\log_{10}$ CFU/mL from 7.6 $\log_{10}$ CFU/mL with 30s treatment of sodium hypochlorite (35 mg/L available chlorine concentration, pH not specified) (Quan et al., 2010). In another study, the planktonic cells were treated with sodium hypochlorite (81 mg/L available chlorine concentration, pH 10.8) for 3 min, with no cells detectable from an initial cell concentration of 7.85 $\log_{10}$ CFU/mL (Chen et al., 2016). For sodium hypochlorite efficacy for killing biofilm cells on biotic surfaces, Roy et al. (2021) assessed 5 min sodium hypochlorite treatment (50, 100, 200, and 300 mg/L, pH not specified) reduced *V. parahaemolyticus* biofilm cells from

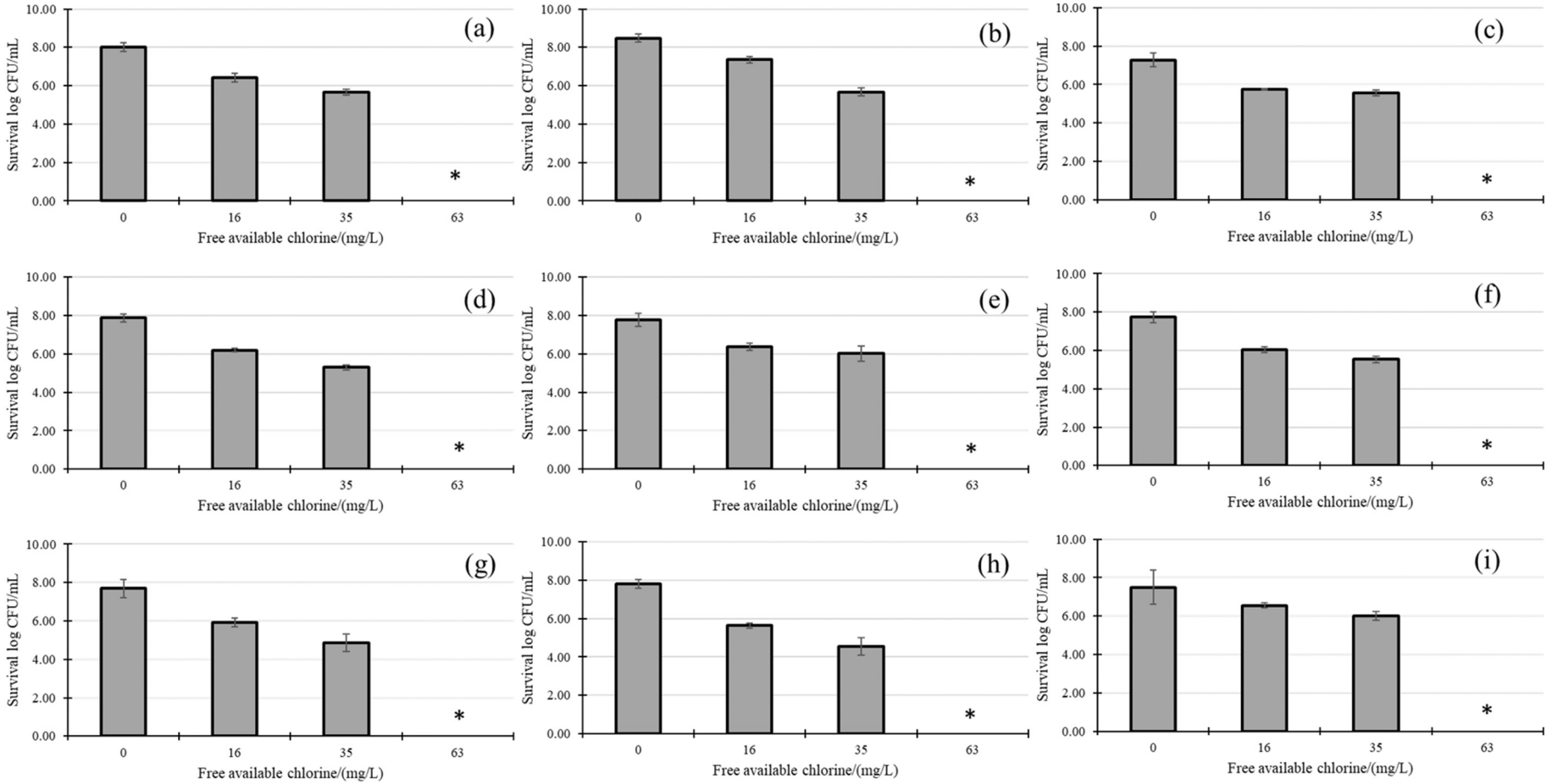


**Fig. 4.** Susceptibility of planktonic *V. parahaemolyticus* to sodium hypochlorite. The indications for strains are as follows: (a) PFR21C03, (b) PFR24B07, (c) PFR29A04, (d) PFR30G02, (e) PFR30J09, (f) PFR34B02, (g) PFR37C06, (h) PFR37D08 and (i) PFR37E03. * indicates the limit of CFU detection (< 10 CFU/mL). Data results presented as mean ± SD.

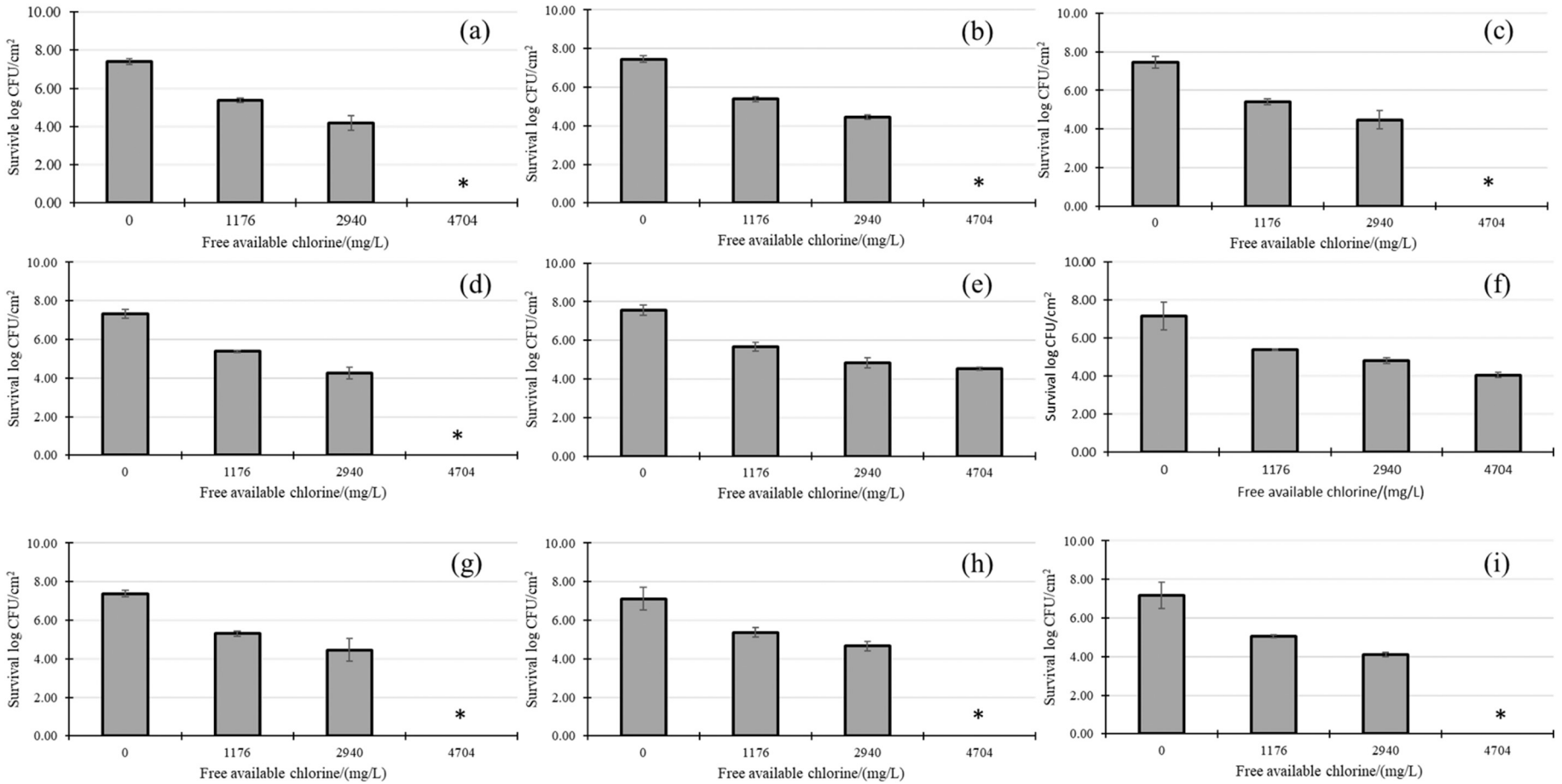


**Fig. 5.** Susceptibility of *V. parahaemolyticus* biofilms to sodium hypochlorite. The indications for strains are as follows: (a) PFR21C03, (b) PFR24B07, (c) PFR29A04, (d) PFR30G02, (e) PFR30J09, (f) PFR34B02, (g) PFR37C06, (h) PFR37D08 and (i) PFR37E03. * indicates the limit of CFU detection (< 10 CFU/mL). Data results presented as mean ± SD.

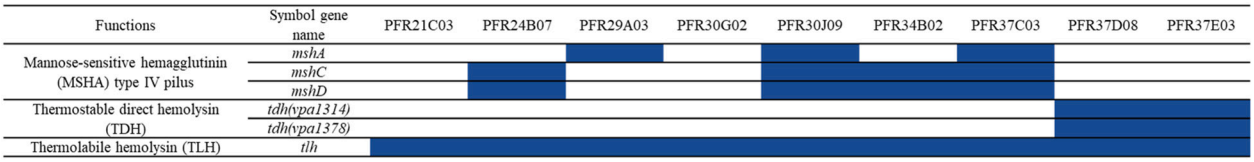


**Fig. 6.** Genetic diversity of biofilm-forming genes in *V. parahaemolyticus* isolates. The presence and absence of biofilm-forming related genes; the blue represents the presence of the gene, white represents the absence.

**Table 1**
Information of strains applied in this study.

| Strains | MLST ST | Nearest ST match (loci hits) | *dnaE* | *gyrB* | *recA* | *dtdS* | *pntA* | *pyrC* | *tnaA* |
|---|---|---|---|---|---|---|---|---|---|
| PFR21C03 | 2632 | – | *dnaE (226)* | *gyrB (25)* | *recA (97)* | *dtdS (19)* | *pntA (26)* | *pyrC (49)* | *tnaA (26)* |
| PFR24B07 | New ST | 2651(6) | *dnaE (175)* | *gyrB (235)* | *recA (3)* | *dtdS (85)* | *pntA (65)* | *pyrC (~68)* | *tnaA (23)* |
| PFR29A04 | 1357 | – | *dnaE (162)* | *gyrB (399)* | *recA (80)* | *dtdS (150)* | *pntA (11)* | *pyrC (158)* | *tnaA (51)* |
| PFR30G02 | 1772 | – | *dnaE (47)* | *gyrB (287)* | *recA (19)* | *dtdS (252)* | *pntA (245)* | *pyrC (18)* | *tnaA (217)* |
| PFR30J09 | New ST | 2650(3) | *dnaE (60)* | *gyrB (406)* | *recA (366)* | *dtdS (390)* | *pntA (18)* | *pyrC (94)* | *tnaA (47)* |
| PFR34B02 | New ST | 2648(6) | *dnaE (36)* | *gyrB (4)* | *recA (81)* | *dtdS (27)* | *pntA (26)* | *pyrC (82)* | *tnaA (225)* |
| PFR37C06 | New ST | 2650(5) | *dnaE (60)* | *gyrB (406)* | *recA (257)* | *dtdS (390)* | *pntA (~156)* | *pyrC (221)* | *tnaA (47)* |
| PFR37D08 | 36 | – | *dnaE (21)* | *gyrB (15)* | *recA (1)* | *dtdS (23)* | *pntA (23)* | *pyrC (~21)* | *tnaA (16)* |
| PFR37E03 | 1140 | – | *dnaE (19)* | *gyrB (295)* | *recA (295)* | *dtdS (223)* | *pntA (136)* | *pyrC (11)* | *tnaA (13)* |

In this table, *dnaE*, *gyrB*, *recA*, *dtdS*, *pntA*, *pyrC* and *tnaA* are housekeeping genes in *V. parahaemolyticus*, and distinct parameters reflect their varied multilocus sequence typing (MLST) information. All 7 housekeeping loci matched with the PubMLST database otherwise, nearest match and loci hit numbers were shown above.

0.54 to 2.59 and 0.64 to 2.32 $\log_{10}$ CFU/cm$^2$ on shrimp and crab surfaces, respectively, from initial concentrations of 6.87 and 7.37 $\log_{10}$ CFU/cm$^2$.

The concentrations of sodium hypochlorite required to eliminate biofilm cells have been determined in many species. Corcoran et al. (2014) reported 500 mg/L sodium hypochlorite was not effective against *Salmonella* biofilm, with a reduction of 1.11 $\log_{10}$ CFU/coupon after 90 min treatment. Cruz and Fletcher (2012) reported 3600 mg/L chlorine as the minimal effective concentration (99.999 % reduction) against L. *monocytogenes* biofilm cells. For *E. coli* O157:H7 attached to rind surfaces for 2 h, a $>5$ $\log_{10}$ reduction occurred after treatment with 2000 mg/L of sodium hypochlorite. For 12 h old biofilms, 2000 mg/L could only achieve a 1.86 $\log_{10}$ reduction (Fu et al., 2017). The effect of sodium hypochlorite on biofilms is dependent on the variants, the age of the biofilm, the structure of the biofilm matrix, the chlorine concentrations, pH and treatment time (Yuan et al., 2021).

In the present trial on biofilm cells, the strong biofilm formers PFR30J09 and PFR34B02 required a greater chlorine concentration, possibly due to more polysaccharide production and a more organised matrix architecture. Similarly, Danese et al. (2000) reported the polysaccharide colonic acid is critical for the complex three-dimensional structure and depth of biofilms in *E. coli* K-12. In *Staphylococcus aureus*, the presence and expression of the gene *ica*, which encodes the polysaccharide poly-*N*-acetylglucosamine (PNAG), are credited with maintaining the integrity of the biofilm architecture and it's resistance to biocidal compounds (Schwartz et al., 2012). Brauge et al. (2018) identified the absence of *N*-acetylglucosamine in teichoic acids caused less adhesion onto surfaces and modified biofilm architecture in L. *monocytogenes*, thereby reducing tolerance to rinsing and cleaning procedures in seafood environments. A relationship between higher resistance and more polysaccharide production was suggested in this study. This could result from the effect on the structure of the matrix causing difficult in sodium hypochlorite to diffuse into or break down the biofilm.

Mature *V. parahaemolyticus* biofilm formation requires type IV pili (mannose-sensitive haemagglutinin type IV pili, MSHA and chitin-regulated pili, ChiRP), EPS biosynthesis and secretion as well as other regulatory factors. Based on the presence and absence of biofilm-forming related genes in this study, the differences among sequenced *V. parahaemolyticus* genomes were mainly located at the *msh* gene clusters that encode MSHA in *V. parahaemolyticus* and TLH toxin producing genes. MSHA has been reported to be required for early attachment to abiotic surfaces. In *V. cholerae*, the *mshA* deficient cells cannot perform cell aggregation though they form three dimensional structures (Moorthy and Watnick, 2004). In *V. parahaemolyticus*, *mshA* mutants of *V. parahaemolyticus* exhibited a lower ability to adhere to surfaces (Shime-Hattori et al., 2006; Williams et al., 2014). Similar results were found for *V. fisheries*, mutants of *mshA* or *mshN* genes in that they were defective for biofilm formation (Visick et al., 2013). Our study indicated that, PFR30J09, the strongest biofilm-forming strain, did not exhibit deficiencies in any of the following genes: *mshA*, *mshC* or *mshD*. In contrast, the weak biofilm forming strains, PFR21C03 and PFR37D08, showed an absence of these three genes. PFR34B02 showed stronger resistance against sodium hypochlorite but did not have the *mshA* gene, indicating that there were other factors responsible for the high EPS production and this requires further investigation. MSHA is modulated by *c*-di-GMP and MshE has as a high-affinity for the *c*-di-GMP receptor (Floyd et al., 2020), suggesting the possibility of using it to interfere with colonization and biofilm development of *V. parahaemolyticus*.

The TDH (encoded by the *tdh* gene) and the TDH-related hemolysin (TRH, encoded by *trh* gene) are primarily associated with pathogenicity, while TLH was reported to be associated with a cytotoxic effect in *V. parahaemolyticus* (Paria et al., 2021). The pathogenicity of *V. parahaemolyticus* may also influence biofilm production but this has not been proven. In the seafood industry, Song et al. (2017) discovered that pathogenic *V. parahaemolyticus* accumulates more biofilm matrix than non-pathogenic strains. Similarly, Wong et al. (2002) found that clinical strains adhered to stainless steel more readily than environmental strains. Though in our study, the pathogenic isolate PFR37D08 was categorized as a weak biofilm former, which might be due to the lack of a host signal/compound and thus the incompetency to incur the strong biofilm forming ability. This result was in consistent with those by Kadam et al. (2013) and Doijad et al. (2015).

Apart from capsular polysaccharide A (CPSA)-a major known component of the *V. parahaemolyticus* biofilm, *vp1476–1458* is an ortholog of the *syp* locus conserved in *V. fischeri,* which is responsible for *syp*-polysaccharide production however this has not been demonstrated for *V. parahaemolyticus* (Yildiz and Visick, 2009). However, the fluorescence microscopy result suggested other β-linked polysaccharides resulted in the biofilm differences among weak and strong biofilm-forming strains but have not this needs further examination.

**Table 2**
Biofilm-forming genes selected to examine in this study.

| Subject_RIMD2210633 | Gene locus | Symbol gene name | Functions |
|---|---|---|---|
| WP_005478391.1 | *vpa1403* | *cpsA* | CPS polysaccharide |
| WP_005478164.1 | *vpa1404* | *cpsB* | |
| WP_005463089.1 | *vpa1405* | *cpsC* | |
| WP_005478193.1 | *vpa1407* | *cpsE* | |
| WP_005478388.1 | *vpa1408* | *cpsF* | |
| WP_005478236.1 | *vpa1409* | *cpsG* | |
| WP_005478215.1 | *vpa1410* | *cpsH* | |
| WP_005478165.1 | *vpa1411* | *cpsI* | |
| WP_005478324.1 | *vpa1412* | *cpsJ* | |
| WP_005465330.1 | *vp0132* | *epsC* | Type II secretion system |
| WP_005478663.1 | *vp0133* | *epsD* | |
| WP_005478662.1 | *vp0134* | *epsE* | |
| WP_005465194.1 | *vp0135* | *epsF* | |
| WP_005465191.1 | *vpa0136* | *epsG* | |
| WP_005461161.1 | *vp0137* | *epsH* | |
| WP_005478722.1 | *vp0138* | *epsI* | |
| WP_005465187.1 | *vp0139* | *epsJ* | |
| WP_005478666.1 | *vp0140* | *epsK* | |
| WP_005458997.1 | *vp0141* | *epsL* | |
| WP_005458943.1 | *vp0142* | *epsM* | |
| WP_005459010.1 | *vp0143* | *epsN* | |
| WP_005480168.1 | *vpa1598* | *gbpA* | Colonization factor GbpA |
| WP_011106342.1 | *vpa0747* | *mshA* | Mannose-sensitive |
| WP_005481001.1 | *vp2696* | *mshC* | hemagglutinin (MSHA type |
| WP_005481015.1 | *vp2695* | *mshD* | IV pilus) |
| WP_005456306.1 | *vp2701* | *mshE* | |
| WP_005456302.1 | *vp2699* | *mshF* | |
| WP_005456304.1 | *vp2700* | *mshG* | |
| WP_011106082.1 | *vp2708* | *mshH* | |
| WP_005481017.1 | *vp2707* | *mshI* | |
| WP_005456325.1 | *vp2706* | *mshJ* | |
| WP_005481006.1 | *vp2705* | *mshK* | |
| WP_005456314.1 | *vp2704* | *mshL* | |
| WP_005456312.1 | *vp2703* | *mshM* | |
| WP_005480990.1 | *vp2702* | *mshN* | |
| WP_005479695.1 | *vp2524* | *pilB* | Type IV-A pilus |
| WP_005479682.1 | *vp2525* | *pilC* | |
| WP_005490359.1 | *vp2526* | *pilD* | |
| WP_005483463.1 | *vp1463* | *sypN* | *syp*-like polysaccharide |
| WP_005454817.1 | *vp1476* | *sypA* | |
| WP_005491469.1 | *vp1475* | *sypB* | |
| WP_005483457.1 | *vp1474* | *sypC* | |
| WP_005454821.1 | *vp1473* | *sypD* | |
| WP_005454845.1 | *vp1472* | *sypE* | |
| WP_005483461.1 | *vp1469* | *sypH* | |
| WP_005483417.1 | *vp1468* | *sypI* | |
| WP_005483478.1 | *vp1467* | *sypJ* | |
| WP_005483470.1 | *vp1466* | *sypK* | |
| WP_005483422.1 | *vp1465* | *sypL* | |
| WP_005483419.1 | *vp1464* | *sypM* | |
| WP_005483455.1 | *vp1462* | *sypO* | |
| WP_005483418.1 | *vp1461* | *sypP* | |
| WP_005483424.1 | *vp1459* | *sypQ* | |
| WP_005483433.1 | *vp1458* | *sypR* | |
| WP_005463268.1 | *vpa1314* | *tdh* | Thermostable direct |
| WP_005478284.1 | *vpa1378* | *tdh* | hemolysin |
| WP_005481504.1 | *vpa0226* | *tlh* | Thermolabile hemolysin |

**Table 3**
Phenotypes of *V. parahaemolyticus* in motility.

| Group | Swimming capacity (/mm)[a] | Swarming capacity (/mm) |
|---|---|---|
| PFR21C03 | 69.33 ± 17.48 | 38.25 ± 11.88 |
| PFR24B07 | 15.17 ± 2.84 | 55.83 ± 5.58 |
| PFR29A04 | 16.75 ± 1.06 | 22.83 ± 5.97 |
| PFR30G02 | 71.00 ± 15.56 | 45.17 ± 22.41 |
| PFR30J09 | 58.58 ± 30.50 | 60.33 ± 8.25 |
| PFR34B02 | 10.33 ± 0.76 | 27.67 ± 4.07 |
| PFR37C06 | 20.00 ± 6.08 | 28.67 ± 1.89 |
| PFR37D08 | 20.67 ± 10.30 | 32.50 ± 12.28 |
| PFR37E03 | 20.00 ± 2.18 | 38.83 ± 3.82 |
| Correlation coefficient with BFI | 0.0632 | 0.0161 |

[a] Data results presented as mean ± standard deviation (SD).

## 5. Conclusion

In conclusion, the strong biofilm-forming strains identified in this study have novel MLST ST types, which will aid in understanding *V. parahaemolyticus* persistence in environmental conditions, shed light on underlying mechanisms of *V. parahaemolyticus* global spread, and aid in the development of effective pathogen control strategies in the food industry. This study also found that attachment contributed to strong biofilm formation in *V. parahaemolyticus*, suggesting additional genes that might have played roles in EPS production in *V. parahaemolyticus* requiring further investigation. *V. parahaemolyticus* biofilms, as with all microbial biofilms, are complex systems. Mono-specific biofilms formed in static high nutrient conditions were used in our study, nevertheless, multi-species biofilms are prevalent in nature and thrive in environments with flowing nutrients.

## Funding

This study is funded by Massey University, the grant number is P963141222WangD.

## CRediT authorship contribution statement

**Dan Wang:** Conceptualization, Methodology, Investigation, Formal analysis, Writing – original draft, Writing – review & editing. **Graham C. Fletcher:** Resources, Conceptualization, Methodology, Supervision, Writing – review & editing. **Stephen L.W. On:** Conceptualization, Methodology, Supervision, Writing – review & editing. **Jon S. Palmer:** Conceptualization, Methodology, Supervision, Writing – review & editing. **Dragana Gagic:** Conceptualization, Methodology, Supervision, Writing – review & editing. **Steve H. Flint:** Project administration, Resources, Supervision, Conceptualization, Methodology, Writing – review & editing.

## Declaration of competing interest

The authors declare no competing conflicts of interest.

## Data availability

Data will be made available on request.

## Acknowledgements

The authors are grateful to Jaime Martinez-Urtaza and Andy Powell of Centre for Environment, Fisheries, and Aquaculture Science (CEFAS) who provided sequence data.

## References

Abanto, M., Gavilan, R.G., Baker-Austin, C., Gonzalez-Escalona, N., Martinez-Urtaza, J., 2020. Global expansion of Pacific Northwest *Vibrio parahaemolyticus* sequence type 36. Emerg. Infect. Dis. 26, 323–326.

Baker-Austin, C., Stockley, L., Rangdale, R., Martinez-Urtaza, J., 2010. Environmental occurrence and clinical impact of *Vibrio vulnificus* and *Vibrio parahaemolyticus*: a European perspective. Environ. Microbiol. Rep. 2, 7–18.

Baker-Austin, C., Oliver, J.D., Alam, M., Ali, A., Waldor, M.K., Qadri, F., Martinez-Urtaza, J., 2018. *Vibrio spp.* infections. Nat. Rev. Dis. Primers. 4, 8.

Baker-Austin, C., Jenkins, C., Dadzie, J., Mestanza, O., Delgado, E., Powell, A., Bean, T., Martinez-Urtaza, J., 2020. Genomic epidemiology of domestic and travel-associated *Vibrio parahaemolyticus* infections in the UK, 2008–2018. Food Control 115, 107244.

Brauge, T., Faille, C., Sadovskaya, I., Charbit, A., Benezech, T., Shen, Y., Loessner, M.J., Bautista, J.R., Midelet-Bourdin, G., 2018. The absence of N-acetylglucosamine in wall teichoic acids of *Listeria monocytogenes* modifies biofilm architecture and tolerance to rinsing and cleaning procedures. PLoS One 13, e0190879.

Buchfink, B., Reuter, K., Drost, H.G., 2021. Sensitive protein alignments at tree-of-life scale using DIAMOND. Nat. Methods 18, 366–368.

Cai, L.L., Hu, H.J., Lu, Q., Wang, H.H., Xu, X.L., Zhou, G.H., Kang, Z.L., Ma, H.J., 2019. Morphophysiological responses of detached and adhered biofilms of *Pseudomonas fluorescens* to acidic electrolyzed water. Food Microbiol. 82, 89–98.
CDC, 2021. The Cholera and Other Vibrio Illness Surveillance (COVIS) System. US Department of Health and Human Services, CDC.
Chen, T.-Y., Kuo, S.-H., Chen, S.-T., Hwang, D.-F., 2016. Differential proteomics to explore the inhibitory effects of acidic, slightly acidic electrolysed water and sodium hypochlorite solution on *Vibrio parahaemolyticus*. Food Chem. 194, 529–537.
Chiba, K., Kawakami, K., Tohyama, K., 1998. Simultaneous evaluation of cell viability by neutral red, MTT and crystal violet staining assays of the same cells. Toxicol. in Vitro 12, 251–258.
Corcoran, M., Morris, D., De Lappe, N., O'Connor, J., Lalor, P., Dockery, P., Cormican, M., 2014. Commonly used disinfectants fail to eradicate *Salmonella enterica* biofilms from food contact surface materials. Appl. Environ. Microbiol. 80, 1507–1514.
Cruz, C.D., Fletcher, G.C., 2012. Assessing manufacturers' recommended concentrations of commercial sanitizers on inactivation of *Listeria monocytogenes*. Food Control 26, 194–199.
Cruz, C.D., Hedderley, D., Fletcher, G.C., 2015. Long-term study of *Vibrio parahaemolyticus* prevalence and distribution in New Zealand shellfish. Appl. Environ. Microbiol. 81, 2320–2327.
Danese, P.N., Pratt, L.A., Kolter, R., 2000. Exopolysaccharide production is required for development of *Escherichia coli* K-12 biofilm architecture. J. Bacteriol. 182, 3593–3596.
Daniels, N.A., Ray, B., Easton, A., Marano, N., Kahn, E., McShan II, A.L., Del Rosario, L., Baldwin, T., Kingsley, M.A., Puhr, N.D., Wells, J.G., Angulo, F.J., 2000. Emergence of a new *Vibrio parahaemolyticus* serotype in raw oysters: a prevention quandary. JAMA 284, 1541–1545.
Di Bonaventura, G., Piccolomini, R., Paludi, D., D'Orio, V., Vergara, A., Conter, M., Ianieri, A., 2008. Influence of temperature on biofilm formation by *Listeria monocytogenes* on various food-contact surfaces: relationship with motility and cell surface hydrophobicity. J. Appl. Microbiol. 104, 1552–1561.
Doijad, S.P., Barbuddhe, S.B., Garg, S., Poharkar, K.V., Kalorey, D.R., Kurkure, N.V., Rawool, D.B., Chakraborty, T., 2015. Biofilm-forming abilities of *Listeria monocytogenes* serotypes isolated from different sources. PLoS One 10, e0137046.
Fang, Y., Visvalingam, J., Zhang, P., Yang, X., 2022. Biofilm formation by Non-O157 Shiga toxin-producing *Escherichia coli* in monocultures and co-cultures with meat processing surface bacteria. Food Microbiol. 102, 103902.
FAO, 2021. Advances in science and risk assessment tools for *Vibrio parahaemolyticus* and *V. vulnificus* associated with seafood: meeting report. https://www.who.int/publications/i/item/9789240024878.
Floyd, K.A., Lee, C.K., Xian, W., Nametalla, M., Valentine, A., Crair, B., Zhu, S., Hughes, H.Q., Chlebek, J.L., Wu, D.C., Hwan Park, J., Farhat, A.M., Lomba, C.J., Ellison, C.K., Brun, Y.V., Campos-Gomez, J., Dalia, A.B., Liu, J., Biais, N., Wong, G.C. L., Yildiz, F.H., 2020. C-di-GMP modulates type IV MSHA pilus retraction and surface attachment in *Vibrio cholerae*. Nat. Commun. 11, 1549.
Fu, Y., Deering, A.J., Bhunia, A.K., Yao, Y., 2017. Biofilm of *Escherichia coli* O157:H7 on cantaloupe surface is resistant to lauroyl arginate ethyl and sodium hypochlorite. Int. J. Food Microbiol. 260, 11–16.
Gurevich, A., Saveliev, V., Vyahhi, N., Tesler, G., 2013. QUAST: quality assessment tool for genome assemblies. Bioinformatics 29, 1072–1075.
Hayrapetyan, H., Muller, L., Tempelaars, M., Abee, T., Nierop Groot, M., 2015. Comparative analysis of biofilm formation by *Bacillus cereus* reference strains and undomesticated food isolates and the effect of free iron. Int. J. Food Microbiol. 200, 72–79.
Jolley, K.A., Bray, J.E., Maiden, M.C.J., 2018. Open-access bacterial population genomics: BIGSdb software, the PubMLST.Org website and their applications. Wellcome Open Res. 3, 124.
Kadam, S.R., den Besten, H.M., van der Veen, S., Zwietering, M.H., Moezelaar, R., Abee, T., 2013. Diversity assessment of *Listeria monocytogenes* biofilm formation: impact of growth condition, serotype and strain origin. Int. J. Food Microbiol. 165, 259–264.
Kaneko, T., Colwell, R.R., 1975. Adsorption of *Vibrio parahaemolyticus* onto chitin and copepods. Appl. Microbiol. 29, 269–274.
Kim, Y.K., McCarter, L.L., 2000. Analysis of the polar flagellar gene system of *Vibrio parahaemolyticus*. J. Bacteriol. 182, 3693–3704.
Lucero-Mejia, J.E., Romero-Gomez, S.J., Hernandez-Iturriaga, M., 2020. A new classification criterion for the biofilm formation index: a study of the biofilm dynamics of pathogenic *Vibrio* species isolated from seafood and food contact surfaces. J. Food Sci. 85, 2491–2497.
Martinez-Urtaza, J., Trinanes, J., Abanto, M., Lozano-Leon, A., Llovo-Taboada, J., Garcia-Campello, M., Pousa, A., Powell, A., Baker-Austin, C., Gonzalez-Escalona, N., 2018. Epidemic dynamics of *Vibrio parahaemolyticus* illness in a hotspot of disease emergence, Galicia, Spain. Emerg. Infect. Dis. 24, 852–859.
Mizan, M.F., Jahid, I.K., Kim, M., Lee, K.H., Kim, T.J., Ha, S.D., 2016. Variability in biofilm formation correlates with hydrophobicity and quorum sensing among *Vibrio parahaemolyticus* isolates from food contact surfaces and the distribution of the genes involved in biofilm formation. Biofouling 32, 497–509.
Moorthy, S., Watnick, P.I., 2004. Genetic evidence that the *Vibrio cholerae* monolayer is a distinct stage in biofilm development. Mol. Microbiol. 52, 573–587.
Nair, G.B., Ramamurthy, T., Bhattacharya, S.K., Dutta, B., Takeda, Y., Sack, D.A., 2007. Global dissemination of *Vibrio parahaemolyticus* serotype O3:K6 and its serovariants. Clin. Microbiol. Rev. 20, 39–48.
Naves, P., del Prado, G., Huelves, L., Gracia, M., Ruiz, V., Blanco, J., Rodríguez-Cerrato, V., Ponte, M.C., Soriano, F., 2008. Measurement of biofilm formation by clinical isolates of *Escherichia coli* is method-dependent. J. Appl. Microbiol. 105, 585–590.
Paria, P., Behera, B.K., Mohapatra, P.K.D., Parida, P.K., 2021. Virulence factor genes and comparative pathogenicity study of *tdh*, *trh* and tlh positive *Vibrio parahaemolyticus* strains isolated from whiteleg shrimp, *Litopenaeus vannamei* (Boone, 1931) in India. Infect. Genet. Evol. 95, 105083.
Parks, D.H., Imelfort, M., Skennerton, C.T., Hugenholtz, P., Tyson, G.W., 2015. CheckM: assessing the quality of microbial genomes recovered from isolates, single cells, and metagenomes. Genome Res. 25, 1043–1055.
Petit III, R.A., Read, T.D., 2020. Bactopia: a flexible pipeline for complete analysis of bacterial genomes. mSystems 5 e00190-00120.
Quan, Y., Choi, K.-D., Chung, D., Shin, I.-S., 2010. Evaluation of bactericidal activity of weakly acidic electrolyzed water (WAEW) against *Vibrio vulnificus* and *Vibrio parahaemolyticus*. Int. J. Food Microbiol. 136, 255–260.
Rosa, J.V., Conceição, N.V., Conceição, R.C.S., Timm, C., 2018. Biofilm formation by *Vibrio parahaemolyticus* on different surfaces and its resistance to sodium hypochlorite. Cienc. Rural 48.
Roy, P.K., Mizan, M.F.R., Hossain, M.I., Han, N., Nahar, S., Ashrafudoulla, M., Toushik, S. H., Shim, W.B., Kim, Y.M., Ha, S.D., 2021. Elimination of *Vibrio parahaemolyticus* biofilms on crab and shrimp surfaces using ultraviolet C irradiation coupled with sodium hypochlorite and slightly acidic electrolyzed water. Food Control 128, 108179.
Schwartz, K., Syed, A.K., Stephenson, R.E., Rickard, A.H., Boles, B.R., 2012. Functional amyloids composed of phenol soluble modulins stabilize *Staphylococcus aureus* biofilms. PLoS Pathog. 8, e1002744.
Sheikh, J., Hicks, S., Dall'Agnol, M., Phillips, A.D., Nataro, J.P., 2001. Roles for fis and YafK in biofilm formation by enteroaggregative *Escherichia coli*. Mol. Microbiol. 41, 983–997.
Shikongo-Nambabi, M.N.N.N., Kachigunda, B., Venter, S.N., 2010. Evaluation of oxidising disinfectants to control *Vibrio* biofilms in treated seawater used for fish processing. Water SA 36, 215–220.
Shime-Hattori, A., Iida, T., Arita, M., Park, K.S., Kodama, T., Honda, T., 2006. Two type IV pili of *Vibrio parahaemolyticus* play different roles in biofilm formation. FEMS Microbiol. Lett. 264, 89–97.
Song, X., Ma, Y., Fu, J., Zhao, A., Guo, Z., Malakar, P., Yingjie, P., Zhao, Y., 2017. Effect of temperature on pathogenic and non-pathogenic *Vibrio parahaemolyticus* biofilm formation. Food Control 73, 485–491.
Sybiya Vasantha Packiavathy, I.A., Agilandeswari, P., Musthafa, K.S., Karutha Pandian, S., Veera Ravi, A., 2012. Antibiofilm and quorum sensing inhibitory potential of Cuminum cyminum and its secondary metabolite methyl eugenol against Gram negative bacterial pathogens. Food Res. Int. 45, 85–92.
Visick, K.L., Quirke, K.P., McEwen, S.M., 2013. Arabinose induces pellicle formation by *Vibrio fischeri*. Appl. Environ. Microbiol. 79, 2069–2080.
Wadhwa, N., Berg, H.C., 2022. Bacterial motility: machinery and mechanisms. Nat. Rev. Microbiol. 20, 161–173.
Wang, D., Flint, S.H., Palmer, J.S., Gagic, D., Fletcher, G.C., On, S.L., 2022. Global expansion of *Vibrio parahaemolyticus* threatens the seafood industry: perspective on controlling its biofilm formation. LWT 158, 113182.
Williams, T.C., Ayrapetyan, M., Oliver, J.D., 2014. Implications of chitin attachment for the environmental persistence and clinical nature of the human pathogen *Vibrio vulnificus*. Appl. Environ. Microbiol. 80, 1580–1587.
Wong, H.C., Chung, Y.C., Yu, J.A., 2002. Attachment and inactivation of *Vibrio parahaemolyticus* on stainless steel and glass surface. Food Microbiol. 19, 341–350.
Yildiz, F.H., Visick, K.L., 2009. *Vibrio* biofilms: so much the same yet so different. Trends Microbiol. 17, 109–118.
Yuan, L., Sadiq, F.A., Wang, N., Yang, Z., He, G., 2021. Recent advances in understanding the control of disinfectant-resistant biofilms by hurdle technology in the food industry. Crit. Rev. Food Sci. Nutr. 61, 3876–3891.
Zheng, S.J., Brook, M.A., 2021. Elastomeric silicone sponges for bleach delivery. ACS Appl. Polym. Mater. 3, 2045–2053.